 doi:10.20944/preprints202112.0436.v1

Type of the Paper (Article)

Reaction Center of Rhodobacter Sphaeroides, a photoactive protein for pH sensing: a theoretical investigation of charge transport properties

Eleonora Alfinito [1,*], and Lino Reggiani[2]

[1] Dipartimento di Matematica e Fisica, "Ennio De Giorgi", Università del Salento; eleonora.alfinito@unisalento.it
[2] Dipartimento di Matematica e Fisica, "Ennio De Giorgi", Università del Salento; lino.reggiani@unisalento.it
* Correspondence: eleonora.alfinito@unisalento.it;

Featured Application: Bio-electronic devices take advantages of some specific duties of biological matter. The specific ability of some proteins to use sunlight is considered for the realization of photo-electronic devices . Here the focus is on the role of the pH, whose variations seem to affect the protein conductance

In the perspective of an even more green trend in science and technology, it is of interest to design devices based on architectures of modular, low cost, and low-pollutant elements, each of them able to perform simple duties. Elemental devices may be themselves green as, for example, proteins able to make simple actions, like sensing. Photosensitive proteins are often considered to this aim because of the possibility of transferring their specific reaction to visible light into electronic signals. The expected electrical response of the photoactive protein Reaction Center (b*RC*) of *Rhodobacter Sphaeroides* is investigated within the proteotronics, a recent branch of molecular electronics that evaluates the electrical properties of a protein by using an impedance network protein analog (INPA) based on its tertiary structure. To this purpose, the linear and nonlinear regimes of the electrical response to an applied bias are studied when the protein is in dark or in the presence of a red light.
Results evidence a significant difference in the electrical properties of b*RC* when the pH value of the solution in which the protein is embedded is changed, in particular from acid to alkaline. These results are in qualitative good-agreement with experimental results reported in the recent literature and strongly suggest the use of this protein as a bio-rheostat or a pH sensor.

Keywords: photosensitive protein; electrical response; theoretical modelling; CAFM; EIS

1. Introduction

In the last few years, bioelectronics, i.e. the branch of electronics which conjugates biological and inorganic matter, is assuming a relevant role in Green Technology. Besides the speculative interest of investigating with electronic/electrochemical methods how biological matter interacts with the environment, a major interest in bioelectronics is to suit some peculiar abilities of living matter (for example, to identify some specific molecules, to detect and use light, and so on) for practical applications, from energy harvesting to sensing action. In this framework, even more biomolecules, mainly proteins and aptamers, have been selected, produced and analyzed with different experimental and theoretical techniques to be part of electronic devices [1-4].

Photosensitive proteins are able to convert electromagnetic energy into different forms of energy useful for their surviving. In particular, after illumination, proteins involved in photosynthesis inside the cell activate an electron transfer that, in turns, activates the ATP-ADP cycle transformations, also producing a proton pumping across the cell membrane [4]. Due to their specific abilities in charge transfer, these proteins are expected to exhibit a better conductivity with respect to other photosensitive proteins. This is the case of type I opsins, which do not transfer electrons after illumination, but simply implement an ion pumping. As a consequence, proteins involved in photosynthesis are among the most studied proteins for electrical/electronic applications [6-8].

Both experimental and theoretical investigations are in progress to shed light on the intriguing mechanisms behind biomolecule activation. In particular, among the different theoretical modelling, proteotronics aims to mimic the set of microscopic mechanisms which, inside the biomolecule, regulate its behavior [9]. Within this framework, charge transport in bacterial Reaction Center (b*RC*) of *Rhodobacter Sphaeroides* is here investigated with the purposes of interpreting available data and suggesting new fields of applications. Specifically, the analysis concerns with some structures of b*RC* deposited in the protein data bank [10], and obtained in different conditions of pH [11].

All proteins, and in general living matter, continuously interact with their environment, i.e. they are open systems. As a consequence, the task of providing a comprehensive model is still far from present possibilities. As an example, temperature, hydration and, of course, the presence of specific ligands, sensitively affect the protein stability and activity, producing a very complex framework of energy landscapes. Indeed, the protein structure is the result of an amino acids sequence (primary structure) which arranges to reach a minimum of the free energy, thus competing with entropy [12]. This means that thousands of equivalent structures should be explored before a short list of the most reliable could be obtained. From one side, the scenario of protein energy states is quite complex and not still complete; it assumes that after folding the protein lives in the ground state of an energy funnel, in which it assumes the most stable configuration. From another side, it is not clear to what extent the configuration is stable with respect the variation of different environmental conditions, or if a degeneracy in energy exists with different proteins living in different equivalent auto-states [13]. The activation (due to energy/ligand binding) should shift the protein toward a different, inequivalent, energy funnel [14]. Waiting for a conclusive description we can only argue in terms of the statistically most relevant structure as given, for example, by the crystallographic investigation (which produces the output after many crystal analysis) and that strictly refers to specific environmental conditions. When these conditions change also the output changes, often in a way which is poorly appreciable at the naked eye but which can induce severe transformation in the protein functioning. Photosensitive proteins are quite interesting in this respect, because the topological transformation they undergo after they have absorbed light energy can appear quite small but produce an indisputable change in their functioning, which has been detected, for example, as an increase of their conductance [15-17]. Due to the difficulty in performing protein crystallization and analysis, available data refer often to a specific combination of environmental conditions and a comparative analysis of the effects of tuning these data is quite difficult to be found.

Anyway, reduced, coarse grained models could capture the system dynamics in at least selected sets of environmental conditions. It is reasonable to suppose that an analysis of the protein around a minimum of the free energy, performed by producing small perturbations of only one significant variable, should drive the protein in a sub-manifold of energy states mainly ruled by that variable. Accordingly, in the present analysis, we focus on the role of pH on proteins in the native state (without illumination) and in the same temperature conditions, which should reduce the contribution of thermal fluctuations. Results are affected by these conditions and the possibility that at higher temperatures thermal fluctuations plays a significant role cannot be excluded.

Proteins are affected by hydration, from the very initial stages of folding to the establishment of the native configuration and eventually of the active configuration [18,19].

Preprints (www.preprints.org) | NOT PEER-REVIEWED | Posted: 27 December 2021 doi:10.20944/preprints202112.0436.v1

Therefore it is not surprising that a relevant change in the amount of H^+ cations in the solution in which b*RC* is present could suffice to arise the electrostatic field around the protein thus inducing a rearrangement of the electrically exposed surfaces. This phenomenon is of great practical interest since the conformational change of the protein structure induces a change of its electrical properties. Therefore, it becomes of relevant interest to investigate these conformational changes and evaluate their electrical effects in the perspective of their applications to electronic devices. To this purpose, the role of pH is here investigated with the objective to find a correlation with an electrical response that, at this stage, can also serve to explore the protein structure. As previously mentioned, the energy state of the protein, and therefore of its conformation, depends on the environmental conditions. While it is easy to understand that, at least in the physiological range, the lowering of the temperature pushes a protein toward its minimum of energy, an analogue trend of the pH value is not *apriori* established. It is even not clear to what extent temperature and pH may influence each other. Starting from a set of data coming from crystallographic investigations performed on b*RC* at different values of pH at the same temperature of 100 °K [11], the present investigation allows a clear separation of the effects of temperature and pH, thus avoiding possible effects of correlated influences.

Investigations on the electrical performances of biomolecules have a long tradition and cover different methodologies. Results of particular interest come from the electrochemical impedance spectroscopy (EIS), and the Conductive Atomic Force Microscopy (CAFM). The former one mainly performs analysis on macroscopic samples (typically with active surfaces of some cm^2) in strong coupling with a buffer/electrolytic solution and in the presence of weak ac applied voltage. Results account for both the sample and solution response and it is in general not easy to discriminate the contributes to the total impedance. Electronic models are continuously updated to give a macroscopic interpretation of the very complex chemical processes [20, 21] . As a matter of fact, many devices, for example sensors, are characterized by the EIS technique, therefore the modelling of results is relevant for both the speculative and applicative aspect [22]. Experiments performed with the EIS technique detect a sensitive enhancement of the cell conductance in light [17, 21]. Specifically, it was observed that the charge transfer involves the protein, the quinones in solution and also depends on the electrode. Furthermore, a sensitive magnification of conductance is observed in light.

CAFM can measure currents from a few to a single biomolecule appropriately bound on a conductive substrate in the presence of significant strong and DC electric fields. Also in this case, the experimental setup plays an important role in the final result, for example, the specific protein anchoring [12], or the measurement mode (for example, contact or tapping mode) [15-16,23]. Photosensitive proteins sandwiched between an electrode and the CAFM tip have been studied under different conditions of illumination showing, in dark, an unexpectedly high conductance [12,23], which can be further enhanced in the presence of light [15].

Concerning the theoretical interpretation of experimental results we make reference to the proteotronics, a recent branch of molecular electronics we have recently developed and that evaluates the electrical properties of a protein by using an impedance network analog based on the protein tertiary structure [9, 24]. By using this approach we succeeded to reproduce and interpret experimental data performed in neutral or quasi-neutral pH condition, and also foresee the results in alkaline conditions. In particular, the results of the investigation predict an increase of conductance in analogy to that given by illumination, and that can be useful for applications in the area of sensor devices.

Preprints (www.preprints.org) | NOT PEER-REVIEWED | Posted: 27 December 2021 doi:10.20944/preprints202112.0436.v1

2. Materials and Methods

2.1. Reaction Center from Rhodobacter Sphaeroides

Proteins arrange their amino acids in a primary, secondary, tertiary and quaternary structure, where: primary indicates the sequence of amino acids, from an N terminus to a C terminus, secondary indicates the organization in helices, sheets or bonds, tertiary indicates the space organization and, finally, when more than one identical protein concur to functioning, quaternary indicates the organization among different proteins. Hereinafter, we use the term structure to make reference to the tertiary structure of the protein which, being sensitive to environmental transformations is the object of the present investigation.

The b*RC* structures of concerns are obtained from crystallographic studies performed in different conditions of illumination and pH (see Table 1). By using these structures, our objective is to determine the electrical response of the single macromolecule as representative of the specific experimental arrangements of the macroscopic device.

bRC is part of the photosynthetic unit, a set of proteins, pigments, and inorganic molecules which harvest and transform energy from light. Specifically, b*RC* mediates a charge separation and transfer inside the cell, involving a couple of quinones (primary and secondary) to which electrons are transferred. Finally, protons are pumped outside the cell membrane. In performing this activity, the protein adapts its structure to the new function, this reshaping being called conformational change.

In performing experiments with proteins that have a well-defined structure, the outcome depends on the orientation they take on the layer on which were deposited [7,12]. As a matter of facts, the orientation of b*RC* in the host cell maximizes its performances by arranging its three chains, say H, L, M, in a cylindrical symmetry, elongating from the Periplasm to the Cytoplasm [11, 12]. Chains L and M extend across the cell membrane while chain H mainly faces the cytoplasmic side and only one helix parallels the other two chains.

When this symmetry is accounted for in experiments that try to reproduce the natural functioning of this protein, the results are amplified [7]. Indeed, the protein arrangement fulfills a transmembrane electron transfer which goes with a proton pumping and proceeds along the protein axes.

In Ref. [11] the role of pH on structure conformation has been analyzed, mainly with respect to the relative orientation of the secondary quinone, and a large set of structures were deposited in the Protein Data Bank (PDB) [10]; some of them are accounted for in the present study.

2.2. Theory

The electrical properties of the b*RC* are investigated making use of the 3D structures listed in Table I, describing the single protein crystallized in different values of pH, both in dark and light.

Table 1. List of the analyzed b*RC* structures. Each structure is identified by a code in the Protein Data Bank [10,11]; illumination conditions and the pH value of the solution in which they were crystallized are reported. The values of the barrier height used for calculations, as well as of the link resistivity are reported.

PDB code	illumination	pH	Φ(meV)	ρ(ΩÅ)
2uww	no	6.5	0.219	$2.7\ 10^{12}$-$5.4\ 10^{10}$
2uws	yes	6.5	0.206-0.219	$2.7\ 10^{12}$
2j8c	no	8.0	0.219	$2.7\ 10^{12}$
2ux3	no	9.0	0.219	$2.7\ 10^{12}$
2uxj	no	10	0.219	$2.7\ 10^{12}$

Preprints (www.preprints.org) | NOT PEER-REVIEWED | Posted: 27 December 2021 doi:10.20944/preprints202112.0436.v1

To this purpose, firstly we analyze the linear impedance response as a function of the frequency under a small applied voltage, typically of a few mV, and represented by Nyquist and Bode plots that can be measured through a standard EIS technique. Secondly, we analyze the static current-voltage (I-V) characteristics of a typical nanostructure at increasing values of applied voltages, up to a few Volts, where deviations from-linear regimes can be achieved by means of a standard CAFM technique.

In brief, the single protein is represented by a set of nodes, one for each considered amino acid, identified by its C_α atom, and a set of links, each connecting a couple of nodes when their distance, $l_{j,k}$, is below an appropriate cut-off value, D [9,24]. In this way, the complete graph representing the single protein is described by a Boolean matrix, $B_{j,k}$= 1/0 corresponding to the presence or any of a link between j and k nodes. The role of the medium (lipids, water molecules, ions, etc.) surrounding the protein is here only indirectly accounted for. Indeed, the medium is involved in the conformational change (for example, when the temperature grows the protein may denature, or when a specific ligand is added in the solution the protein may change its conformation, or, as explored in the present investigation, when the amount of cations grows, the protein shrinks its structure) and its effects are resumed in the protein conformation.

For the calculations of the electrical properties, each link is interpreted as a channel for charge transfer whose impedance $Z_{j,k}$ is taken to be a function of the geometry, of the link resistivity ρ, and of the intrinsic polarizability $\varepsilon_{j,k}$ of j, k amino acids as in [24]

$$Z_{j,k} = \frac{l_{j,k}}{A_{j,k}(\rho^{-1} + i\varepsilon_{j,k}\varepsilon_0\omega)} \qquad (1)$$

where

$$A_{j,k} = \frac{\pi\left(D^2 - {l_{j,k}}^2\right)}{4} \qquad (2)$$

is the cross-sectional area shared by the labeled amino acids, ε_0 the vacuum dielectric constant, ω the angular frequency and i the imaginary unit. The value of ρ is taken to be the same for all the amino acids, unless differently specified in the following.

The resulting impedance network preserves the features of the protein that are relevant for calculations, i.e., the amino acid positions and their electrical properties. By using Kirchhoff laws, the charge transfer inside the network is described by a set of linear equations that are solved by a standard numerical procedure. The solution so obtained provides the electrical response of the network in terms of its local currents and voltage drops, its global impedance and/or its static I-V characteristics. We remark that different 3D structures produce different electrical outputs which can be compared with what found in experiments performed in light and in dark on some opsins i.e., bacteriorhodopsin, bR, or proteorhodopsin, pR [15-16, 23]. There, a marked difference of the electrical characteristics was observed because of the conformational change induced by the presence of light or other specific ligands [14,25-28]

3. Results

The theoretical model refers to a single protein taken as representative of the macroscopic electrical response. The role played by the position of the contacts can be of relevance for the results of both experiment and theory. As a consequence, within a first estimate, we will consider two possible contact geometries, a first up-down as in the cell arrangement, and a second tilted of π/2, as it can happen in a nonhomogeneous sample and is visualized in Figure 1.

Preprints (www.preprints.org) | NOT PEER-REVIEWED | Posted: 27 December 2021 doi:10.20944/preprints202112.0436.v1

(a) **(b)**

Figure 1. Cartoon of b*RC* with different positions of the electrical contacts. On the left, **(a)** the up-down configuration with the "IN" contact on the cytoplasmic side and the "out" contact on the periplasmic side. On the right, (b), the transverse configuration, with both contacts on the periplasmic side. In both cases, the "IN" contact is on the H chain, but on different helices.

While sensitive structural differences are not impressive to the naked eye, they appear more clearly when the network analysis is performed. As an example, in Figure 2 we report the set of contacts which characterize the structure in dark at two different pH values. Elements on the diagonal correspond to sequential amino-acids. This figure shows that the main differences between the pH 6.5-structure and the pH 10-structure is mainly due to the position of sequential amino-acids. As a matter of facts, at pH=6.5 more contacts appear on chain H while at pH 10 more contacts are on chains L and M. In other terms, by increasing the pH the protein deforms from bottom to up, thus becoming more tight toward the periplasmic side.

In the following we investigate two charge-transport regimes that are usually considered by experiments. To this purpose, a first subsection is devoted to the linear response regime, typically adopted within the EIS technique, and a second subsection is devoted to the non-linear transport regime, typically adopted within the CAFM technique. We assume as a benchmark the b*RC* structure in dark at pH =6.5 (PDB code 2uww), as well as its impedance value.

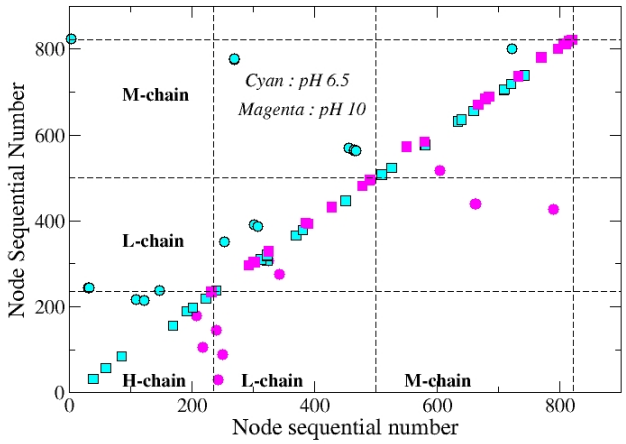

Figure 2. Differential contact maps of the b*RC* in dark with two different values of pH. Circles (squares) describe the contacts which are specific for the configuration. Data are calculated using *D*=6 Å.

Preprints (www.preprints.org) | NOT PEER-REVIEWED | Posted: 27 December 2021 doi:10.20944/preprints202112.0436.v1

3.1. Linear response regime

Under linear response regime all the parameters entering the local impedance in Equation 1 do not depend on the applied bias. Accordingly, Figure 3 reports the normalized resistance of the single protein in dark, R(#)/R, i.e. the static (DC, i.e., ω=0) global resistance R(#) of the protein, normalized to the benchmark value R, in dark, as a function of the cut-off distance between neighborhood nodes, *D*. In particular, the protein at pH = 10 (PDB code 2uxj) is compared with the protein at pH = 6.5 (PDB code 2uww). Calculations have been performed by using two different contact configurations as reported in Figure1.

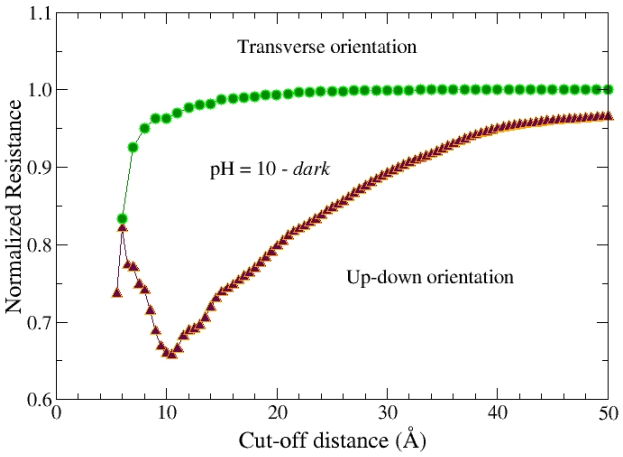

Figure 3. The normalized -resistance R(#)/R of b*RC* at pH=10, as a function of the cut-off distance *D* . Data are obtained using different contact orientations: the up-down in which the protein is assumed to be with the chain H (but helix 1) on the electrode (see Figure 1a), and the transverse one in which the protein lays on its back on the electrode (see Figure 1b). Data refer to structures in dark.

From the above comparison we conclude that the value of the pH plays a significant role only in the up-down orientation, where the value of the resistance stays well below that of the benchmark. By using the up-down orientation, Figure 4 reports the normalized resistance of the single protein , R(#)/R, calculated at different values of pH. A higher sensitivity is observed at increasing values of pH. In particular, the best resolution is observed for the value *D* = 10.5 Å of the cut-off distance, that compares well with the value *D* = 6 Å found for the case of bacteriorhodopsin (bR), a protein similar to b*RC* but with a smaller number of amino acids for about a factor of 4 [14]. In the inset of Figure 4 the resistance of the protein in light at pH 6.5 is compared with the benchmark resistance. Also in this case, the maximal resolution shows up for a cut-off value *D*=10.5 Å, with a reduction of resistance in fair agreement with experiments [12].

Preprints (www.preprints.org) | NOT PEER-REVIEWED | Posted: 27 December 2021 doi:10.20944/preprints202112.0436.v1

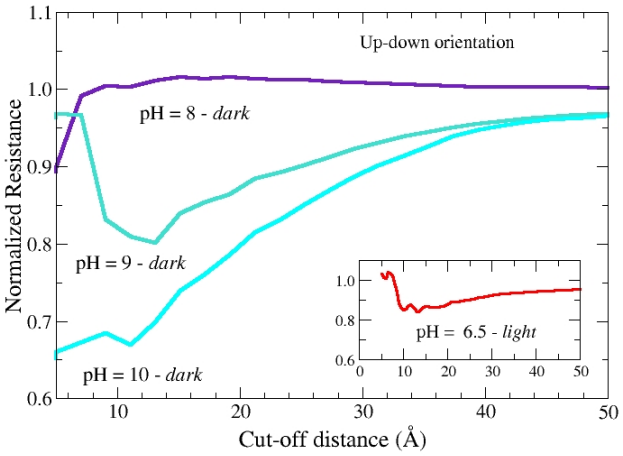

Figure 4. The normalized resistance R(#)/R of b*RC* in dark, as a function of the cut-off distance between neighborhood nodes, *D*, at different values of pH. Calculations refer to up-down orientation and three different pH values. The inset reports the normalized resistance R(#)/R in light for pH =6.5.

Finally, making use of the up-down orientation in dark, and taking $\rho = 2.7\ 10^{12}\ \Omega$ Å we evaluate the complete impedance spectra for pH = 6.5 and 10 respectively, in the frequency range (10^{-2}-10^{4} Hz) which covers the full experimental range. In this range, experiments detect the solution effects, mainly at the highest frequencies, and the electrode resistance, at the lowest frequencies. Otherwise, all the cell elements contribute to the global impedance response in the full frequency range [20, 21]. The impedance model may be more or less complex to account several effects that could be detected by experiments. Anyway, the main contribution is given by Equation (1) and accounts for both the polarization and some leakage currents which are usually present in real dielectrics [9,21]. In an electrochemical cell conduction has both an electronic and ionic origin, i.e. charge may travel through both organic/inorganic matter and also the electrolytic solution. Furthermore, charge may accumulate between different solid/liquid or solid/solid interfaces [21]. Equation (1) describes an elemental circuit consisting of a resistance (R) and a capacitor (C) in parallel, R//C, and its graphical representations in terms of frequency are called Bode plots. The imaginary vs the real part of impedance is represented by the so-called Nyquist plot. Calculated Nyquist and Bode plots could be attributed to an ideal single R//C circuit (see Figure 5), which means that the elemental R//C circuits in the protein (each of them representing a single link) exhibit a synchronous response. In other terms, a single relaxation time is detected, the same for both configurations, $\tau = 0.015$ s. This value is compatible with the experimental data reported in the literature [21]. Having the configurations different geometries also their elemental capacitances exhibit different values that are larger for the case of a pH =10, in fair agreement with the observation of a more tight shape with respect to the pH= 6.5 configuration.

Preprints (www.preprints.org) | NOT PEER-REVIEWED | Posted: 27 December 2021 doi:10.20944/preprints202112.0436.v1

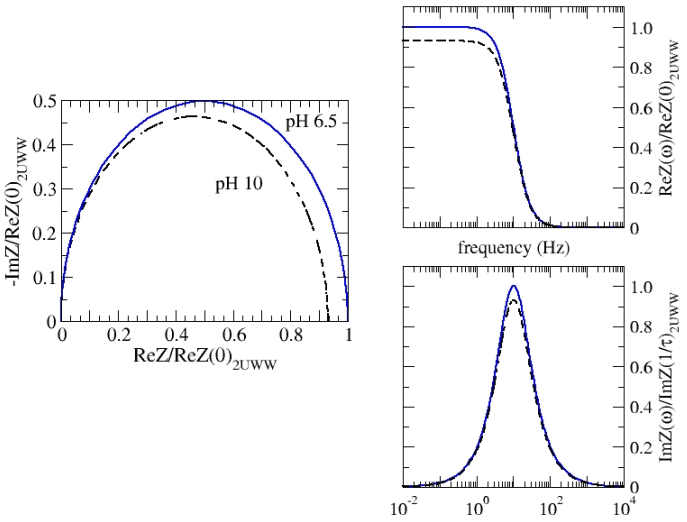

Figure 5. Nyquist (on the left) and Bode (on the right) plots of the b*RC* normalized-impedance. Calculations refer to the single protein in the up-down orientation in dark, with pH=6.5 (continuous line) and pH=10 (dashed line). Calculations have been performed using ρ=2.7 10^{12} Ω Å and *D*=10.5Å

3.2. Super-linear response regime

To reproduce the super-linear behavior exhibited by the current-voltage *(I-V)* experiments obtained with a CAFM technique, at increasing values of an applied positive-voltage [12], the microscopic model makes use of a sequential tunneling mechanism of charge transfer between different nodes that are assumed to be separated by an energy barrier Φ. Accordingly, the link resistivity, $\rho_{j,k}$ is chosen to depend on the local voltage drop $V_{j,k}$ between the couple of *j,k* amino acids involved in the link, as:

$$\rho_{j,k} = \begin{cases} \rho_{max} , & if \quad eV_{j,k} \leq \Phi \\ \rho_{max}\left(\frac{\Phi}{eV_{j,k}}\right) + \rho_{min}\left(1 - \frac{\Phi}{eV_{j,k}}\right), & if \quad eV_{j,k} \geq \Phi \end{cases} \qquad (3)$$

Specifically, the current response is simulated by using a Monte Carlo procedure to allow the charge transfer channels to reduce their initial resistivity from a ρ_{max} value to a ρ_{min} value at increasing of the potential drop between nodes [14, 25-28]. This is on the wake of the well-known Simmons model for the charge injection in an electronic junction [29]. Indeed, the model describes two different tunneling regimes: at low bias it envisages a direct tunneling mechanism, at high bias overtaken by an injection tunneling mechanism. At low bias, the condition $eV_{j,k} \leq \Phi$ holds for most of the channels that take the same ρ_{max} value, thus the global response of the protein is similar to that of a high resistance Ohmic conductor. At increasing bias, $eV_{j,k} \geq \Phi$, an abrupt drop of the resistivity to the minimal value, ρ_{min} , occurs for the given channel and the global resistance of the protein will decrease accordingly. At further increasing of the bias, most of the channels will take the ρ_{min} value and the global response of the protein will be similar to that of a low resistance Ohmic conductor. The tunneling transition probabilities including direct, ${\mathcal{P}_{j,k}}^{D}$, and injection, or Fowler Nordheim (FN), mechanisms, ${\mathcal{P}_{j,k}}^{FN}$, writes:

$${\mathcal{P}_{j,k}}^{D} = \exp\left[-\left(\frac{2l_{j,k}\sqrt{2m}}{\hbar}\right)\sqrt{\left(\Phi - \frac{eV_{j,k}}{2}\right)}\right] \quad if \quad eV_{j,k} \leq \Phi, \qquad (4)$$

$${\mathcal{P}_{j,k}}^{FN} = \exp\left[-\left(\frac{2l_{j,k}\sqrt{2m}}{\hbar}\right)\frac{\Phi^{3/2}}{\sqrt{2}eV_{j,k}}\right] \quad if \quad eV_{j,k} \leq \Phi, \qquad (5)$$

Preprints (www.preprints.org) | NOT PEER-REVIEWED | Posted: 27 December 2021 doi:10.20944/preprints202112.0436.v1

where $\hbar$ is the reduced Planck constant, e is the unit charge, and m is the electron effective mass, here taken the same of the bare value.
Current-voltage characteristics under different conditions are reported in the following Figures 6 to 8.

By using up-down and transverse orientations, Figure 6 compares the *I-V* characteristics of b*RC* in dark, at pH = 6.5 and 10. Furthermore, in the up-down orientation, the *I-V* characteristics of b*RC* in dark and light at pH = 6.5 are compared. The current response of the up-down orientation is found to be of about 2 orders of magnitude higher than that of the transverse orientation.. The sensitivity to the increase of pH is small for the transverse orientation. while it goes up to about 50 % for the case of the up-down orientation (at 1 Volt). Calculations use the following parameters: ρ_{max} = 2.7 10^{12} Ω Å, ρ_{min}= 2.7 10^{4} Ω Å and Φ = 0.219 eV .These data confirm that the primary role of contact position does not disappear in the super-ohmic regime.

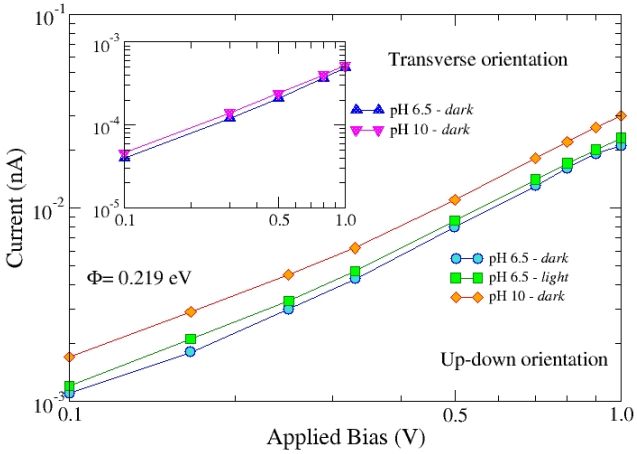

Figure 6. *I-V* characteristics of b*RC* in dark and in light within a range of applied bias of interest for experiments. The contacts are in the up-down orientation. Circles refer to results with the protein in dark at pH = 6.5, squares refer to the protein in light at pH = 6.5, diamonds refer to the protein in dark at pH = 10. In the inset the I-V characteristics are for the protein in dark at pH = 6.5 (triangle up) and at pH = 10 (triangle down) using contacts in the transverse orientation. Lines are guides for the eye. Calculations make use of the following parameters: D = 10.5 Å, ρ_{max} =2.7 10^{12} Ω Å, ρ_{min} =2.7 10^{4} Ω Å, Φ = 0.219 eV.

Figure 7 reports the *I-V* characteristics of b*RC* in the up-down in dark orientation and in light at pH = 6.5 for a range of applied bias of interest for experiments.

Calculations make use of three values for the barrier height, Φ = 0.219 eV (squares), Φ = 0.212 eV (diamonds), and Φ = 0.206 eV (triangles). Even a small decrease of the barrier height is found to be responsible for a significant increase of the current in light above about 0.7 V , due to the anticipated onset of tunneling in the FN regime. By contrast, for the same value of the barrier height the results in light and in dark are practically the same.

These result support the idea that in b*RC* the conformational change due to illumination is not the main cause of the observed current enhancement; instead, we can suppose that the energy received by light is transferred to the electrons which, finally, cross an effective barrier smaller than that measured in dark. Still a small variation (here smaller than 6%) is sufficient for producing a consistent enhancement of the current.

Preprints (www.preprints.org) | NOT PEER-REVIEWED | Posted: 27 December 2021 doi:10.20944/preprints202112.0436.v1

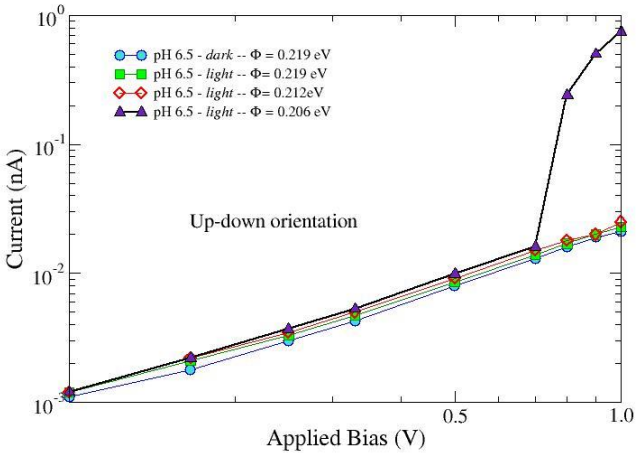

Figure 7. *I-V* characteristics of b*RC* in dark and in light within a range of applied bias of interest for experiments. The contacts are in the up-down orientation. Calculations are performed by using three different value of the barrier height, Φ = 0.219 eV (squares), Φ = 0.212 eV (diamonds), and Φ = 0.206 eV (triangles). Circles refer to the protein in dark, with data calculated assuming Φ = 0.219 eV. Lines are guides for the eye.

Figure 8 reports the *I-V* characteristics calculated in dark at pH = 6.5 for the protein in the up-down orientation (symbols) and are compared with experiments [12], (continuous lines). In these experiments, performed with the CAFM, the protein was immobilized on an Au-electrode and contacted with the CAFM tip. Both the electrode and the tip have been coated with different chemicals. Here we focused on three different assembly, say, Au/4MP/protein/Au, Au/2MP/protein/Au and Au/2MP/protein/2MP/Au, where 2MP indicates 2-mercaptopyridine and 4MP 4-mercaptopyridine [12].

The satisfactory agreement between theory and experiments is obtained by using different values for ρ_{max} to account for the different chemical modifiers used to anchor the protein, while keeping the same values for the other parameters. Three different values of ρ_{max} have been used, namely: 2.7 10^{12} Ω Å, 1.2 10^{11} Ω Å and 5.4 10^{12} Ω Å, to fit experiments performed by using, respectively, the Au/4MP/protein/Au, Au/2MP/protein/Au and Au/2MP/protein/2MP/Au, assembly. This result suggests that the role played by the chemical modifiers of the electrode and/or the CAFM tip is to increase the effective conductivity of the protein and it is not due to the change of the potential barrier height. As a matter of facts, the shape of the *I-V* curve is the same for the three cases, while the absolute value is changed. Therefore, the reduced effective conductivity should be due to a better match of the Fermi level of the electrode with the LUMO/HOMO molecular orbitals of the protein, as suggested in Ref. [12]. As a matter of fat,, having carried out the theoretical analysis with the same orientation (up-down), a realignment due to the chemical modifiers seems to be less relevant.

Preprints (www.preprints.org) | NOT PEER-REVIEWED | Posted: 27 December 2021 doi:10.20944/preprints202112.0436.v1

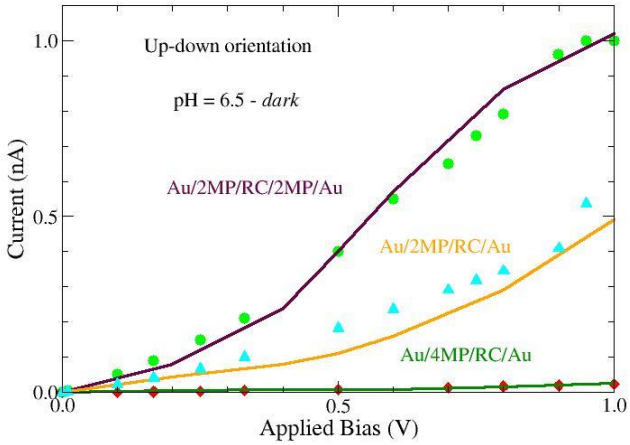

Figure 8. *I-V* characteristics of b*RC* in dark and in light for a range of applied bias of interest for experiments, Φ = 0.219eV. The contacts are in the up-down orientation.. Calculations are performed by using three different values of ρ_{max} = 2.7 10^{12} Ω Å, (red diamonds), ρ_{max} = 2.7 10^{11} Ω Å (cyan triangles), and ρ_{max} = 5.4$10^{10}$ Ω Å (green circles). All the calculations assume ρ_{min} = 2.7 10^{4}Ω Å and Φ = 0.219 eV. Continuous lines refer to experimental data from [12] obtained by using samples in which the protein was sandwiched between differently modified electrodes as reported in the figure.

4. Discussion

By using the tertiary structure of the b*RC* protein, its electrical characteristics are investigated under dark and light conditions and varying the pH of the crystallized solution, ranging from weak acid up to strong alkaline values. Theoretical calculations are carried out in the framework of the proteotronics, a structure-minded approach to the new field of protein-based electronics. The protein has been analyzed in the linear and non-linear regime of electrical response. Specifically, in the linear regime, i.e., at low applied bias, calculations of resistance (DC) and impedance (AC) suggest that b*RC* is extremely sensitive to the pH value of the solution in which it is crystallized. The protein undergoes a resistance reduction when the pH changes from weak acid (pH = 6.5) to alkaline conditions, and by increasing the pH value up to 10 this change appears even more evident. The non-linear regime was investigated, using a Monte Carlo procedure at increasing bias values and different conditions of illumination and pH. The current-voltage characteristics compares well with available experiments performed in quasi-neutral conditions and in dark. This supports the expectations for alkaline and in light conditions.

These kinds of analysis should be of relevance for a future application of these proteins in technology, for example in designing solar energy harvesters. From one side , they highlight the primary role of pH in the detectable electrical responses, which should be accounted for in designing new bio-electronic devices. From another side, they can be used, for example, to regulate resistance in such devices. Finally, the present investigation can be thought as a hint for designing pH-sensors.

Author Contributions: Conceptualization, methodology, validation, writing and editing E.A. and L.R.; software, E.A.. Both authors have read and agreed to the published version of the manuscript.

Conflicts of Interest: The authors declare no conflict of interest.

References

1. Dunn, M. R., Jimenez, R. M., & Chaput, J. C. Analysis of aptamer discovery and technology. *Nature Rev. Chem*. **2017**, *1(10)*, 1-16.
2. Alfinito, E., Reggiani, L., Cataldo, R., De Nunzio, G., Giotta, L., & Guascito, M. R. (2017). Modeling the microscopic electrical properties of thrombin binding aptamer (TBA) for label-free biosensors. Nanotechnology, 28(6), 065502.
3. Tokita, Y., Tamada, S., Luo, W., Goto, Y., Bouley-Ford, N., Nakajima, H. & Watanabe, Y. Protein photoconductors and photodiodes. *Angew. Chem. Int. Ed.* **2011** 50, 11663.
4. Zhang, L., Lu, J. R., & Waigh, T. A. Electronics of peptide-and protein-based biomaterials. *Adv. Colloid Interface Sci.* **2021**,*287*, 102319.
5. Allen, J. P.; Feher, G.; Yeates, T. O.; Komiya, H.; & Rees, D. C. Structure of the reaction center from Rhodobacter sphaeroides R-26: the protein subunits. *PNAS* **1987**,*84(7)*, 6162-616.
6. Das, R.; Kiley, P. J.; Segal, M.; Norville, J.; Yu, A. A.; Wang, L.; ... & Baldo, M. (2004). Integration of photosynthetic protein molecular complexes in solid-state electronic devices. *Nano Letters* **2004** 4(6), 1079-1083.
7. Altamura, E.; Milano, F.; Tangorra, R. R.; Trotta, M.; Omar, O. H.; Stano, P.; & Mavelli, F. Highly oriented photosynthetic reaction centers generate a proton gradient in synthetic protocells, *PNAS*, **2017**114(15), 3837-3842.
8. Sun, J.; Yang, P.; Li, N.; Zhao, M.; Zhang, X.; Zhang, Y.; ... & Lu, X. Extraction of photosynthetic electron from mixed photosynthetic consortium of bacteria and algae towards sustainable bioelectrical energy harvesting.*Electrochim. Acta* **2020** , *336*, 135710.
9. Alfinito, E.; Pousset, J.; & Reggiani, L. *Proteotronics: development of protein-based electronics*; Publisher: Pan Stanford, Boca Raton, Florida; 2015.
10. Berman, H. M.; Westbrook, J.; Feng; Z.; Gilliland, G.; Bhat, T. N.; Weissig, H.; ... and Bourne, P. E. The protein data bank. *Nucl. Acids Res.* **2000** , *28(1)*, 235-242.
11. Koepke, J.; Krammer, E. M.; Klingen, A. R.; Sebban, P.; Ullmann, G. M.; & Fritzsch, G. pH modulates the quinone position in the photosynthetic reaction center from Rhodobacter sphaeroides in the neutral and charge separated states. *J. Mol. Bio.* **2007**, *371(2)*, 396-409.
12. Mikayama, T.; Iida, K.; Suemori, Y.; Dewa, T.; Miyashita, T.; Nango, M.; ... & Cogdell, R. J. The electronic behavior of a photosynthetic reaction center monitored by conductive atomic force microscopy. *J. Nanosci. Nanotechnol***.** **2009** , *9(1)*, 97-107.
13. Onuchic, J. N.; Luthey-Schulten, Z.; & Wolynes, P. G. Theory of protein folding: the energy landscape perspective. *Annu. Rev. Phys. Chem***. 1997**, *48(1)*, 545-600.
14. Alfinito, E.; & Reggiani, L. Mechanisms responsible for the photocurrent in bacteriorhodopsin, Phys. Rev. E. 2015, 91(3) , 032702.
15. Jin, Y.; Friedman, N.; Sheves, M.; He, T.; & Cahen,D. Bacteriorhodopsin (bR) as an electronic conduction medium: Current transport through bR-containing monolayers, *PNAS* **2006**, *103(23)*, 8601-8606.
16. Melikyan, H.; Khishigbadrakh, B. E.; Babajanyan, A.; Lee, K.; Choi, A. R.; Lee, J. H.; ... and Friedman, B. Proteorhodopsin characterization based on metalinsulatormetal structure technique. *Thin Solid Films*. **2011**, 519(10), 3425-3429.
17. Białek, R.; Swainsbury, D. J.; Wiesner, M.; Jones, M. R.; & Gibasiewicz, K. Modelling of the cathodic and anodic photocurrents from Rhodobacter sphaeroides reaction centres immobilized on titanium dioxide. *Photosynth. Res.* **2018**, *138*(1), 103-114.
18. Srivastava, J.; Barber, D. L.; & Jacobson, M. P. Intracellular pH sensors: design principles and functional significance. *Physiology* **2007** , *22* , 30-39.
19. Hou, C.; Zhang, F.; Chen, C.; Zhang, Y.; Wu, R.; Ma, L.; ... & Liu, X. Y. Wearable hydration and pH sensor based on protein film for healthcare monitoring, *Chem. Pap.* **2021** , *75*, 4927-4934.
20. Sacco, A. (2017). Electrochemical impedance spectroscopy: Fundamentals and application in dye-sensitized solar cells. *Renewable and Sustainable Energy Reviews*, *79*, 814-829.
21. Alfinito, E.; Milano, F.; Beccaria, M.; Cataldo, R.; Giotta, L.; Trotta, M.; & Guascito, M. R. A biological-based photovoltaic electrochemical cell: modelling the impedance spectra. *Chemosensors*, **2020** , *8*(1), 20.
22. Bonanos, N., Steele, B. C. H., Butler, E. P., Macdonald, J. R., Johnson, W. B., Worrell, W. L., ... & Eisenberg, R. S. (2018). Applications of impedance spectroscopy. *Impedance spectroscopy: Theory, experiment, and applications*, 175-478.
23. Casuso, I.; Fumagalli, L.; Samitier, J.; Padrós, E.; Reggiani, L.; Akimov, V.; and Gomila, G. Nanoscale electrical conductivity of the purple membrane monolayer . *Phys. Rev. E* **2007**, *76(4)* , 041919.
24. Alfinito, E.; Reggiani, L.; & Pousset, J. Proteotronics: Electronic devices based on proteins. In *Sensors 2015*; Compagnone, D., Baldini,F., Di Natale, C., Betta, G., Siciliano, P. Eds.; Springer, Cham. pp. 3-7.
25. Alfinito, E.; Millithaler, J. F.; & Reggiani, L. Charge transport in purple membrane monolayers: A sequential tunneling approach. *Phys.Rev*.**2011** , *E* 83(4), 042902.
26. Alfinito, E.; Pousset, J.; Reggiani, L.; & Lee, K. Photoreceptors for a light biotransducer: a comparative study of the electrical responses of two (type-1) opsins, *Nanotechnology*, **2013** , *24(39)*, 395501.
27. Alfinito, E.; & Reggiani, L. Modeling current-voltage characteristics of proteorhodopsin and bacteriorhodopsin: Towards an optoelectronics based on proteins, *IEEE Trans. Nanobioscience* **2016** , *15(7)*, 775-780 .
28. Alfinito, E.; & Reggiani, L. Opsin vs opsin: New materials for biotechnological applications. *JAP* , **2014** , *116(6)*, 064901.
29. Simmons, J. G. Generalized formula for the electric tunnel effect between similar electrodes separated by a thin insulating film. *JAP*,**1963**,*34(6)*,1793-1803.